Contents lists available at ScienceDirect

Colloids and Surfaces A: Physicochemical and Engineering Aspects

journal homepage: www.elsevier.com/locate/colsurfa

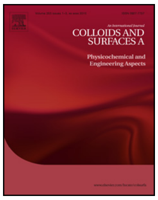

Effect of basicity and sodium ions on stability of polymeric ferric sulfate as coagulants

Dingtian Jia[a], Mingyu Li[a,*], Guoqiang Liu[a], Penghui Wu[a], Jingfang Yang[a], Yichun Li[a], Shaofen Zhong[b], Wenjie Xu[a]

[a] *Water Treatment Engineering Research Center, School of Environment, Jinan University, Guangzhou 510632, China*
[b] *Dongguan Cleaner Production Center, Dongguan University of Technology, Dongguan 523808, China*

HIGHLIGHTS

- Basicity has no effect on the structure and morphology of the precipitates in PFS.
- The precipitates in PFS prepared by $NaClO_3$ were sodium jarosite.
- Na_2SO_4, NaCl and $NaNO_3$ added into PFS significantly decreased the stability of PFS.
- The precipitates in PFS prepared by H_2O_2 added sodium salt were sodium jarosite.
- The existence of sodium ions was an important cause for the instability of PFS.

GRAPHICAL ABSTRACT

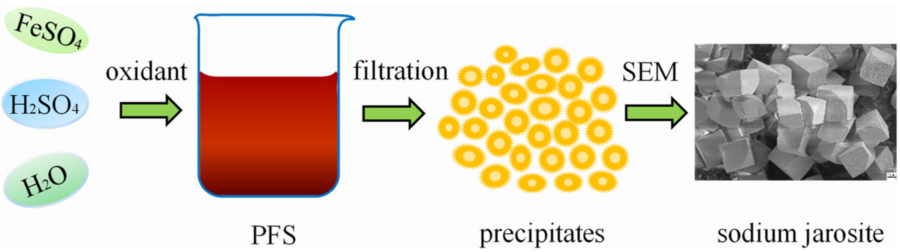

ARTICLE INFO

Article history:
Received 27 July 2016
Received in revised form
27 September 2016
Accepted 11 October 2016
Available online 13 October 2016

Keywords:
Polyferric sulfate
Sodium jarosite
Inorganic polymer coagulant
Basicity
Precipitates

ABSTRACT

In this paper, the stability of polymeric ferric sulfate (PFS) prepared by direct oxidation method was studied. The relationship between Basicity and stability of PFS was investigated and the structure and morphology of the precipitates in PFS were evaluated using Fourier transformed infrared spectroscopy (FTIR), X-ray diffraction (XRD), Thermogravimetric analysis (TG-DTG) and Field emission scanning electron microscopy (FESEM). Considering the existence of sodium ion in PFS prepared by $NaClO_3$, the effects of Na_2SO_4, NaCl and $NaNO_3$ on the stability of PFS were investigated, and the composition and formation mechanism of the precipitates were also probed. The results indicated that the Basicity has no effect on the structure and morphology of the precipitates. The precipitates in PFS prepared by $NaClO_3$ were sodium jarosite. We also found that the Na_2SO_4, NaCl and $NaNO_3$ that added into PFS significantly decreased the stability of PFS. The results also indicated that the precipitates in PFS prepared by H_2O_2 was an amorphous structure containing Fe^{3+}, OH^-, SO_4^{2-}. However, the precipitates in PFS prepared by H_2O_2 added sodium salt were rhombohedra (pseudo cubic) crystals sodium jarosite, which was consisted with the precipitates in PFS prepared by $NaClO_3$. Above all, we concluded that the existence of sodium ions was an important cause for the instability of PFS.

1. Introduction

Iron-based materials widely used in environmental protection, especially their applications for water treatment. For example, nano-iron hydroxide or oxide, which has a strong adsorption

---

* Corresponding author.
E-mail address: tlimy@jnu.edu.cn (M. Li).

http://dx.doi.org/10.1016/j.colsurfa.2016.10.021
0927-7757/

capacity and then with a good removal of organic pollutants [1]. Another example, traditional or polymeric iron salts are considered to be quite effective flocculants, which due to compressed electric double layer mechanism can make colloidal suspensions destabilization and subsequently reach a satisfactory charge neutralization effect. Flocculation (coagulation-flocculation) is one of the important principles of colloid chemistry, which can make the fine particles suspended in the water agglomerate into some large flocs, and then separated from the water. So the flocculation system becomes one of the significant unit operations used in water purification and wastewater treatment. This process is mainly achieved through the addition of inorganic polymeric coagulants. Polymeric ferric sulfate (PFS) is a new type of inorganic polymer coagulants, which is an intermediate compound between ferric sulfate and ferric hydroxide and has a general formula of $[Fe_2(OH)_n(SO_4)_{3-n/2}]_m$ ($n < 2$, $m > 10$) [2]. In the coagulation-flocculation process, PFS can remove the turbidity, colloidal suspensions, COD_{Cr}, color and heavy metals [3–6]. Compared to the conventional Fe-based coagulants, such as $FeCl_3$ and $Fe_2(SO_4)_3$, PFS has a lot of advantages due to a certain degree of cations. For instance, lower effluent turbidity could be obtained when using PFS to treat water and wastewater and low temperature has less adverse effect on its flocculation [7,8]. In addition, PFS has better coagulation performance than other Al-based coagulants such as aluminum sulfate ($Al_2(SO_4)_3$) and polyaluminum chloride (PAC) [9], and the toxicity test demonstrated that potable water treated by PFS is safer than coagulants based on aluminum to human health [10,11].

Many methods were used to prepare PFS in liquid forms. One of the most important methods is direct oxidation process, in which the strong oxidants, such as sodium chlorate, potassium chlorate and hydrogen peroxide, were used to oxidize Fe(II) to Fe(III) [12]. And then Fe(III) was hydrolyzed and polymerized. Due to its comparatively simple process, the relatively short reaction time and the mild reaction conditions, the direct oxidation process is widely used in industrial production.

PFS has some disadvantages, which leads to its lower market share. Since PFS has strong acidity, it can easily decrease the water pH, furtherly destroying the coagulation effect and corrupting the equipment to a certain extent. Therefore, if we can reduce the acidity of PFS, namely preparing the high Basicity PFS, its market share can increased, which has been a hot issue in the field of water treatment agent and industrial production. Basicity (B) is the mass ratio of OH^- to the Fe^{3+} in the PFS, which is linked closely with the stability of PFS. The Basicity is proportional to the degree of polymerization and large number of hydroxyl polymer with a positive charge which can assure satisfactory effects of water treatment. To some extent, this means that the performance and quality of the polymeric ferric sulfate product could be superior. However, PFS products which have the high Basicity ($B > 16\%$), are usually unstable and prone to precipitate, resulting in the deterioration of product's performance and quality. This phenomenon is more likely to occur, when sodium chlorate or potassium chlorate is used as oxidant during the direct oxidation process.

The previous studies focused on the performance of PFS in potable water and wastewater treatment and the PFS preparation methods [13–16]. In addition, the types of oxidant, production equipment and operating conditions, which are used to produce the PFS also have been studied extensively [17–19]. However, few reports were found on the precipitate in the PFS.

In this paper, PFS were prepared by the method of direct oxidation and characterized in regard to representative physical properties, such as pH, density, total iron concentration, ferrous ion concentration and Basicity (B). In addition, the relationship between Basicity and stability of PFS was studied, and the structure and morphology of precipitates in PFS were characterized by Fourier transformed infrared (FTIR) spectrophotometer, X-ray diffraction (XRD), Thermogravimetric analysis (TG-DTG) and Field emission scanning electron microscopy (FESEM). Meanwhile, Na_2SO_4, NaCl, and $NaNO_3$ were added respectively to the PFS prepared by H_2O_2 to investigate the effect of sodium salt on the stability of PFS. Finally, the causes and the mechanism of the instability of PFS were discussed.

2. Material and methods

2.1. Materials and experimental method

All reagents used for samples preparation and analysis in this study are analytically pure chemicals. Unless otherwise specified, all the solutions used in the experiment were prepared with deionized water.

The ferrous sulfate, sulfuric acid and deionized water with the predetermined amounts (see Table 1) were added to a reaction vessel with an agitator. The oxidant (sodium chlorate or hydrogen peroxide) was slowly added to the mixed solutions accompanying by strongly stirring. After the oxidant was added, vigorously stirring was continuously provided until the quantity of ferrous ions in the reaction solution was less than 0.1%, which can be considered that the ferrous sulfate has been oxidized completely. Then the red-brown liquid polymeric ferric sulfate was prepared.

100 mL of the PFS solution was sealed and preserved at ambient temperature and the stability of PFS solution was observed. When the solution had a certain amount of precipitates appeared, then put the precipitates to settle and separated it from the PFS solution by pumping filtration. The separated precipitates were firstly washed several times with sulfuric acid acidification of water ($pH = 2.0–2.5$) and then washed a few times with deionized water until the pH value of the washing solution was close to or reaches neutral. Finally, the precipitates were dried at 110 °C overnight and then stocked in the dryer for further analysis.

2.2. Analysis method

2.2.1. Characterization of PFS

The total iron concentration, ferrous ion concentration, pH, and Basicity (B) of PFS were measured and calculated according to the National Standard of P. R. China for PFS (GB 14591-2006). The Basicity was calculated using Eq. (1).

$$B = [OH^-]/3[Fe] \times 100\% \tag{1}$$

2.2.2. FTIR analysis of the precipitates

1.00–2.00 mg from the dried precipitates were mixed with 250 mg KBr to obtain the analytical samples using the potassium bromide tabletting technique. FTIR spectroscopy was measured by Bruker EQUINOX-55 infrared spectrophotometer and the spectra range from 4000 cm^{-1} to 400 cm^{-1}.

2.2.3. X-ray diffraction of the precipitates

The crystalline phases of precipitates powder were characterized by X-ray diffraction (XRD) using a MSAL-XD2 X-ray diffractometer. The scanning range from 10 to 70° of 2-theta angle at a scan rate of 8°/min with Cu Kα radiation (40 kV, 20 mA, $\lambda = 1.54051$ Å). Before each experimental analysis and determination, X-ray diffractometer using quartz as a standard calibration.

2.2.4. TG-DTG analysis of the precipitates

Thermogravimetric analyses (TG-DTG) was conducted on a Netzsch 209F3 thermal analyzer. The carrier gas was nitrogen flowing at 20 mL/min. Sample masses varied between 10 and 15 mg and was heated in an alumina crucible at a constant ramping of temperature between ambient and 850 °C at a rate of 10 °C/min.

Table 1
Preparation prescription and physical characteristics of PFS prepared from same amounts of $FeSO_4{\cdot}7H_2O$[a].

Run No.	H_2SO_4 (g)	Oxidants(g)		Total iron (wt%)	Density (g/mL)	B (wt%)
		$NaClO_3$	H_2O_2			
1	12.72	6.30		11.05	1.492	5.21
2	10.55	6.30		10.98	1.486	10.08
3	8.29	6.30		11.04	1.475	15.34
4	6.05	6.30		11.03	1.464	20.16
5	3.76	6.30		11.08	1.450	25.57
6	12.72		25.00	11.02	1.490	5.34
7	10.55		25.00	11.05	1.487	9.87
8	8.29		25.00	11.08	1.476	15.64
9	6.05		25.00	10.97	1.463	21.05
10	3.76		25.00	11.04	1.451	25.47

[a] Inputs 83.40 g $FeSO_4{\cdot}7H_2O$.

2.2.5. FESEM analysis of the precipitates

The morphology of the samples of precipitates powder was observed by FESEM using a Zessi Ultra-55 field emission scanning electron microscopy operating at 5 kV.

3. Results and discussion

3.1. Effect of basicity on the stability of PFS

The amounts of two oxidants ($NaClO_3$ or H_2O_2) and the physical characteristics (Total iron concentration, Density, Basicity) of PFS prepared with different quantity of sulfuric acid were showed in Table 1. All the PFS products reached or surpassed the National Standard of P. R. China for PFS (GB 14591-2006). The same quantity of ferrous sulfate was put in all preparation process of PFS, which resulted in the total iron concentration of the PFS of every runs was almost the same (11.0 wt%). The amounts of sulfuric acid and water added to the reactor are slightly different, which is the reason for the difference of density in each run.

PFS samples can be classified according to their stability. PFS samples from runs 1–2 and runs 6–8, respectively, synthesized by $NaClO_3$ and H_2O_2, which have no precipitates occurs in the stored procedure (three months at ambient temperature). PFS samples from runs 3–5, turned turbid after one week, and earth yellow precipitates appeared after 11 days. PFS samples from runs 9–10, appear light brown precipitates after two months. Compared with PFS produced by $NaClO_3$ under the same Basicity conditions, PFS prepared by H_2O_2 had shown better stability. Normally, the higher Basicity of the PFS resulted in worse stability.

3.2. Analysis of precipitates in PFS prepared by $NaClO_3$

3.2.1. FTIR analysis of precipitates

FTIR spectra of the precipitates in PFS of runs 1–5 is presented in Fig. 1. All runs are characterized by similar Fourier spectra, which is reflected in the same wavenumber and intensity of the absorption peaks. In the characteristics bonds at 3300–3500 cm^{-1} and 1638–1641 cm^{-1}, which is considered to the stretching vibration of –OH group and to the bending vibration of water absorbed, polymerized and crystallized in the precipitates [20]. Moreover, the IR peaks at 1184–1190 cm^{-1} and 508–511 cm^{-1} could be assigned to the asymmetric stretching vibration of Fe-O-Fe [21,22]. Additionally, a strong absorption peaks exhibit at 1095–1099 cm^{-1} wavenumber, which are attributed to the Fe-OH-Fe bonds stretching vibrations, indicating that the polymers are formed in the precipitates. The same peaks in the region of 1008–1010 cm^{-1} and can be ascribed to the stretch vibrations of the $S=O$ or the $O=S=O$ bonds. Moreover, the sulphates ($SO_4{}^{2-}$) present a relatively weaker band in the range of 626–629 cm^{-1} [3]. From the FTIR experimental data, we can conclude that no significant difference in the characteristic groups or chemical bonds of the precipitates in PFS of runs 1–5 as all spectra shows analogous peaks of the same wavenumber and intensity.

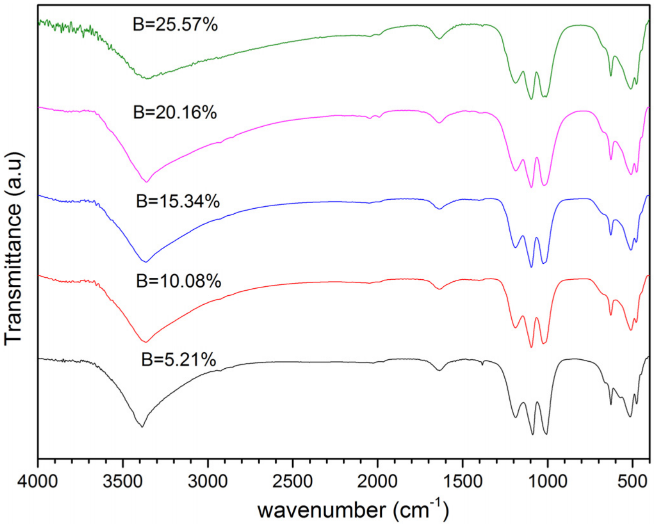

Fig. 1. FTIR spectra of precipitates in PFS of different basicity by oxidation of $NaClO_3$.

3.2.2. XRD analysis of precipitates

X-ray diffraction (XRD) analysis found that the precipitates in PFS of runs 1–5 all had clear diffraction peaks and peak intensity, especially at 2θ of 17.51°, 28.57° and 29.10°, indicating that the precipitates had the same crystal structure. It could be explained that they are the same substance. The X-ray powder diffraction graph is shown in Fig. 2, and the precipitates easily identified by comparison with the diffraction pattern published by International Center for Diffraction Data (ICDD) No.00-036-0425, corresponding to sodium jarosite, the chemical formula for $NaFe_3(SO_4)_2(OH)_6$. Meanwhile, sodium jarosite containing OH^- and $SO_4{}^{2-}$ functional groups, was consistent with Fig. 1 of the precipitates FTIR analysis.

3.2.3. Thermogravimetric analysis of precipitates

In order to study the thermal decomposition process of the precipitates in PFS of runs 1–5, thermal analyzer was performed under nitrogen from ambient temperature up to 850 °C. Similar experimental data were acquired for all precipitates in PFS of runs 1–5 examined, in spite of tiny differences in the temperature and mass loss of some curves were observed. The TG-DTG curves for the precipitates are given in Fig. 3.

Thermal gravimetric (TG) and differential thermal gravimetric (DTG) curves suggested that the breakdown of the precipitates in PFS occurred in three main steps: 220, 378, and 640 °C. The mass

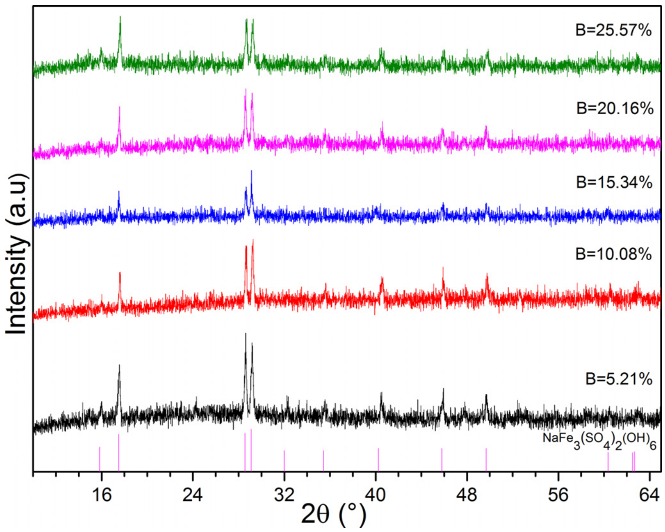

Fig. 2. XRD analysis of precipitates in PFS of different basicity by oxidation of $NaClO_3$.

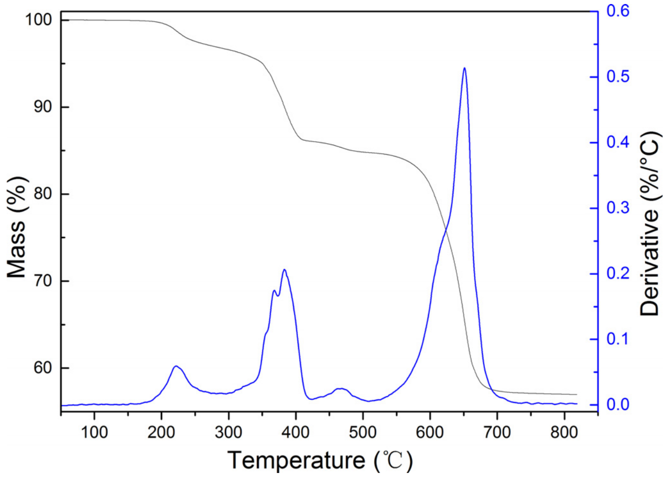

Fig. 3. TG-DTG analysis of precipitates in PFS of different basicity by oxidation of $NaClO_3$.

losses related with these steps are 4.66, 11.35, and 26.63% respectively, and resulted in a total mass loss of 42.64%.

3.2.3.1. Step 1: dehydration. When the precipitates were heated again at 290 °C, no further mass loss was observed and TG curve has a little flat area, suggesting that this is the process of losing the adsorption or crystallization water and the structure of precipitates is temporarily stabilized [23,24]. According to the process of mass loss in TG curve (Fig. 3), the quantity of adsorption or crystallization water can be estimated, and the theoretical amount of adsorption or crystallization water was 1.32 mol. DTG curves suggests that the loss of adsorption or crystallization water occurs at 220 °C, and this process comply with the following equation:

$$NaFe_3(SO_4)_2(OH)_6{\cdot}XH_2O \rightarrow NaFe_3(SO_4)_2(OH)_6 + XH_2O \quad (2)$$

3.2.3.2. Step 2: dehydroxylation. In the second step, the mass loss of 11.35% at 378 °C could be ascribed to the loss of $3H_2O$ from sodium jarosite, which consistent with the theoretical mass loss of 11.13% based on the reaction equation. This was quite possible owing to the dehydroxylation process resulted in the structure breakdown of the sodium jarosite [25,26], which was explained by the following equation:

$$NaFe_3(SO_4)_2(OH)_6 \rightarrow NaFe(SO_4)_2 + Fe_2O_3 + 3H_2O \quad (3)$$

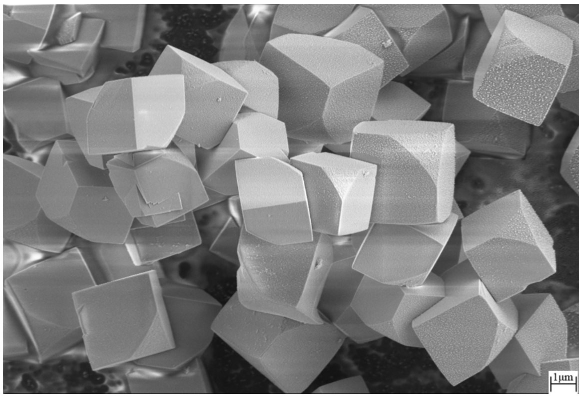

Fig. 4. FESEM images of precipitates in PFS of different basicity by oxidation of $NaClO_3$.

3.2.3.3. Step 3: desulfation. The desulfation reaction take place in 640 °C resulting in the formation of Na_2SO_4 and iron oxide as follows formula [27]:

$$2NaFe(SO_4)_2 \rightarrow Fe_2O_3 + Na_2SO_4 + 3SO_3 \quad (4)$$

The theoretical mass loss in this process was 24.74%, and the actual mass loss was 26.63%. Through the thermal decomposition of the precipitates by TG-DTG analysis, we could make a conclusion that the process of thermal decomposition of the precipitates agreed with sodium jarosite thermal decomposition.

3.2.4. *Morphology of the precipitates*

The results of FTIR and XRD were confirmed by FESEM observations. Field emission scanning electron microscopy (FESEM) was adopted to probe the structure and morphology of the precipitates in PFS. The FESEM morphology picture of the precipitates is shown in Fig. 4. It presents a clear cube and globular rhombohedra shape structure. According to the relevant references on PFS, it was known that the PFS samples showed amorphous structure with tiny traces of crystallinity. It is concluded that the precipitate's structure in PFS prepared by oxidation of $NaClO_3$ is different from the PFS samples, while its morphology is consistent with the sodium jarosite based on relevant references [28].

3.3. *Effect of sodium salt on the stability of PFS*

PFS was prepared by the direct oxidation of sodium chlorate containing H^+, Fe^{3+}, OH^- and $SO_4{}^{2-}$, as well as the presence of Na^+ and Cl^- ions. The study of PFS by oxidation of $NaClO_3$ indicated that the precipitates in PFS are sodium jarosite. This is different from the previous studies. The sodium ion is involved in the formation of the precipitates. However, for the PFS prepared by oxidation of H_2O_2 without Na^+ and Cl^-, the solution only contained H^+, Fe^{3+}, OH^- and $SO_4{}^{2-}$. Therefore, sodium sulfate, sodium chloride and sodium nitrate were respectively added to the PFS (B = 21.05%, run 9) prepared by oxidation of H_2O_2 to study the effect of sodium salt on the stability of PFS. Meanwhile, the PFS prepared by the oxidation of H_2O_2 without added sodium salt was used as blank control. All the PFS solution was sealed for 40 days and preserved at ambient temperature and then the stability of PFS solution was observed. The precipitates in PFS were taken out and characterized by FTIR, XRD, TG-DTG, and FESEM.

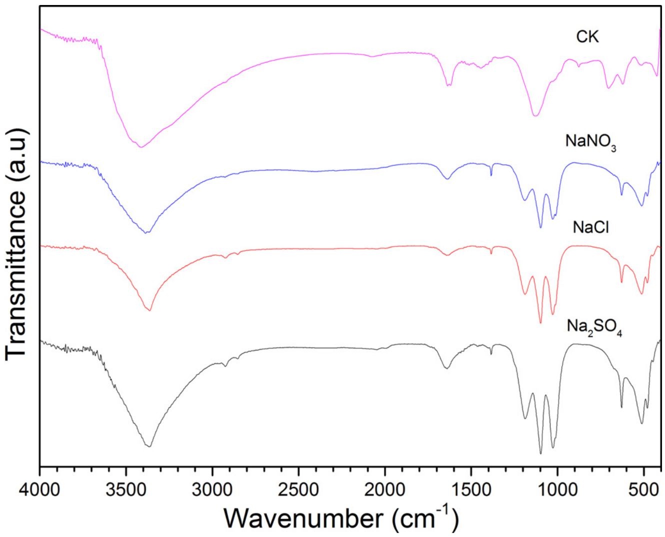

Fig. 5. FTIR spectra of precipitates in PFS added sodium salt.

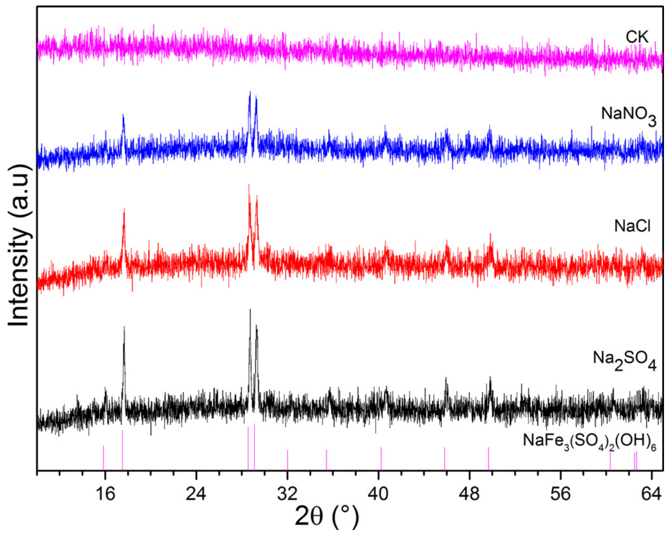

Fig. 6. XRD analysis of precipitates in PFS added sodium salt.

In order to facilitate the presentation of precipitates, we describe it as: (I) precipitates in PFS prepared by oxidation of H_2O_2 without added sodium salt, mark it as CK; (II) precipitates in PFS prepared by oxidation of H_2O_2 with the addition of sodium sulfate, mark it as Na_2SO_4; (III) precipitates in PFS prepared by oxidation of H_2O_2 with addition of sodium chloride, mark it as NaCl and (IV) precipitates in PFS prepared by oxidation of H_2O_2 with addition of sodium chloride, mark it as $NaNO_3$.

3.3.1. *FTIR analysis of precipitates*

FTIR spectra of the precipitates in PFS (B = 21.05%, runs.9) with addition of sodium salt are presented in Fig. 5. The absorption peaks of CK in 1000–1400 cm^{-1} were significantly different from the (II), (III) and (IV). However, the spectra of (II), (III) and (IV) all exhibit two characteristics bonds at 3300–3500 cm^{-1} and 1638–1641 cm^{-1}, which is consistent with the precipitates prepared by $NaClO_3$ (Fig. 1). We can concluded that the precipitates in PFS with sodium salts has the same structure and the precipitates in the PFS with sodium salts is different from the precipitates structure in the CK.

3.3.2. *XRD analysis of precipitates*

XRD analysis of the precipitates in PFS (B = 21.05%, run 9) with addition of sodium salt is presented in Fig. 6. X-ray diffraction (XRD) analysis found that the precipitates in PFS of CK have many diffraction peaks which are the diffuse reflection peaks and large 2θ scan absence of peaks related to crystal structure. However, the precipitates of (II), (III) and (IV) all showing many peaks associated with crystal structure, which comparison with the diffraction pattern published by International Center for Diffraction Data (ICDD) No.00-036-0425, corresponding to sodium jarosite. This is also consistent with the precipitates in PFS by oxidation of $NaClO_3$. Therefore, it can be explained that the existence of sodium salt could promote the formation of precipitates in PFS, resulting in the PFS solution instability.

3.3.3. *Thermogravimetric analysis of precipitates*

The thermal decomposition process of the precipitates in PFS with addition of sodium salt are showed in Fig. 7. The precipitates in PFS without sodium salts (Fig. 7A) had different TG-DTG curves from Fig. 7B that was precipitate samples with added Na_2SO_4. Especially, the DTG curve of Fig. 7B between 300 and 400 °C have clearly peak which was consistent with the curve of precipitates in PFS prepared by $NaClO_3$ in Fig. 3. However, the DTG curve of Fig. 7A in the range of 200–400 °C shows a very slow mass loss process that always occurs in a non-crystalline material, and the TG curves is consistent with the relevant references of PFS prepared by H_2O_2. This phenomenon confirmed that the XRD curve in Fig. 6 of CK did not have clear diffraction peaks. Therefore, the TG-DTG curves confirmed that the precipitates of (I) and (II) were different materials.

3.3.4. *Morphology of the precipitates*

The morphology of the precipitates in PFS with addition of sodium salt is showed in Figs. 8. The precipitates in PFS without sodium salts (Fig. 8A) were comprised of spherical aggregates resembling pincushions structure with very small degrees of crystallinity and diameter of approximately 1 μm. However, Fig. 8B reveals a number of crudely formed rhombohedra (pseudo cubic) crystals of the precipitates in PFS with Na_2SO_4 addition, which was consistent with Figs. 4 of the precipitates in PFS prepared by oxidation of $NaClO_3$ and the precipitates is sodium jarosite. This shows that the sodium ions involved in the process of crystalline transformation, and the existence of sodium ions was an important cause for the instability of PFS.

3.4. *Theoretical inference on the formation of precipitates in PFS*

PFS has a chemical formula, $[Fe_2(OH)_n(SO_4)_{3\text{-}n/2}]_m$, considered as obtained by polymerization of the monomers $Fe_2(OH)_n(SO_4)_{3\text{-}n/2}$. Preparation of PFS process is to oxidize Fe(II) to Fe(III) by strong oxidant, such as $NaClO_3$ or H_2O_2, which is generally expressed as:

$$6FeSO_4 + NaClO_3 + 3(1\text{-}n/2)H_2SO_4 = 3[Fe_2(OH)_n(SO_4)_{3\text{-}n/2}] + 3(1\text{-}n)H_2O + NaCl \quad (5)$$

$$2FeSO_4 + H_2O_2 + (1\text{-}n/2)H_2SO_4 = Fe_2(OH)_n(SO_4)_{3\text{-}n/2} + (2\text{-}n)H_2O \quad (6)$$

When both aci dic conditions and sufficient sodium ions are present (with Na_2SO_4 for example), the following reactions occur:

$$3[Fe_2(OH)_n(SO_4)_{3\text{-}n/2}] + 6H_2O = 3[Fe_2(OH)_{n+2}(SO_4)_{2\text{-}n/2}] + 3\,H_2SO_4 \quad (7)$$

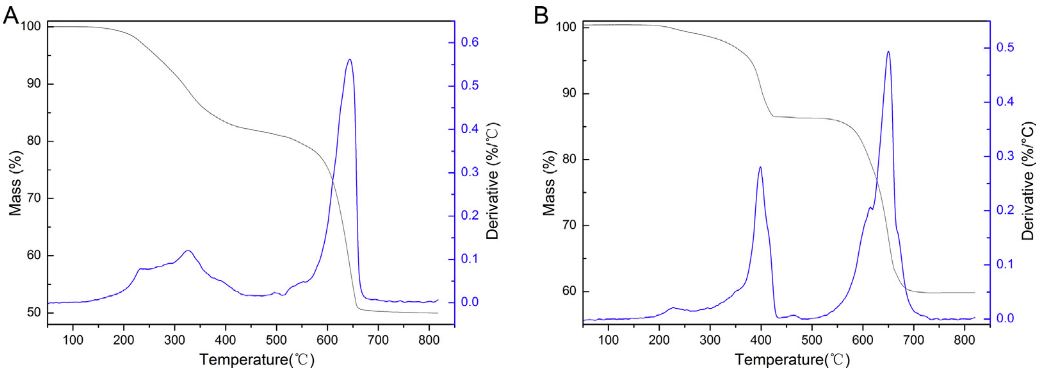

Fig. 7. TG-DTG analysis of precipitates in PFS added sodium salt(A) precipitates in PFS without sodium salts, (B) precipitates in PFS with addition of Na_2SO_4.

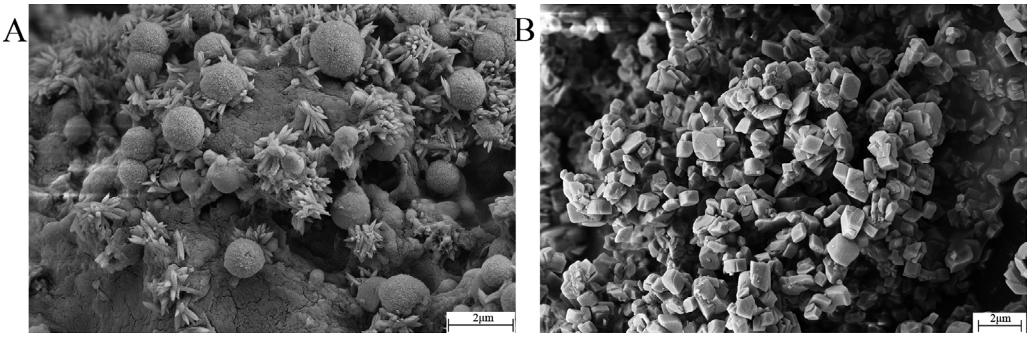

Fig. 8. FESEM images of precipitates in PFS with addition of sodium salt(A) Precipitates in PFS without sodium salts, (B) Precipitates in PFS added Na_2SO_4.

$$3[Fe_2(OH)_{n+2}(SO_4)_{2-n/2}] + Na_2SO_4 + (6\text{-}3n)H_2O = Na_2Fe_6(SO_4)_4(OH)_{12} + (3\text{-}3n/2)H_2SO_4 \quad (8)$$

(7) + (8), the total reaction:

$$3[Fe_2(OH)_n(SO_4)_{3-n/2}] + Na_2SO_4 + (12\text{-}3n)H_2O = Na_2Fe_6(SO_4)_4(OH)_{12} + (6\text{-}3n/2)H_2SO_4 \quad (9)$$

Therefore, the reaction equation indicated that the presence of Na^+ in the PFS will cause the Reaction (8) and (9), resulting in the formation of sodium jarosite and the deterioration of PFS stability. This is also the reason why PFS prepared by oxidation of H_2O_2 is more stable than that prepared by oxidation of $NaClO_3$ under the same basicity conditions.

4. Conclusion

In summary, the results indicated that the Basicity had no effect on the morphology and structure of the precipitates in PFS prepared by $NaClO_3$, which were all sodium jarosite. And also demonstrated that the precipitates in PFS prepared by H_2O_2 contained Fe^{3+}, OH^-, and $SO_4{}^{2-}$ with very small degrees of crystallinity. However, the precipitates in PFS prepared by H_2O_2 with addition of sodium salt were rhombohedra (pseudo cubic) crystals sodium jarosite, which was consistent with the precipitates in PFS prepared by $NaClO_3$. It was concluded that the existence of sodium ions was a significant cause for the instability of PFS. Therefore, this also provides an important theoretical basis for prepare PFS with high B value and good stability, and the sodium ions in the process of industrial production should be avoided.

Acknowledgments

This work was supported by the Major Project of Higher Education Institutes Water Treatment Materials Industry-University-Research Cooperation Demonstration Base of Guangdong Province, China (No. cgzhzd1004), and the Science and Technology Project of Dongguan City, China (No. 2013108101032).

References

[1] J.B. Fei, Y. Cui, J. Zhao, L. Gao, Y. Yang, J.B. Li, Large-scale preparation of 3D self-assembled iron hydroxide and oxide hierarchical nanostructures and their applications for water treatment, J. Mater. Chem. 21 (2011) 11742–11746.

[2] M.H. Fan, S.W. Sung, R.C. Brown, T.D. Wheelock, F.C. Laabs, Synthesis characterization, and coagulation of polymeric ferric sulfate, J. Environ. Eng. ASCE 128 (2002) 483–490.

[3] A.I. Zouboulis, P.A. Moussas, E. Vasilakou, Polyferric sulphate: preparation, characterisation and application in coagulation experiments, J. Hazard. Mater. 155 (2008) 459–468.

[4] J.Q. Jiang, N.J.D. Graham, Observations of the comparative hydrolysis/precipitation behaviour of polyferric sulphate and ferric sulphate, Water Res. 32 (1998) 930–935.

[5] Z.P. Xing, D.Z. Sun, Treatment of antibiotic fermentation wastewater by combined polyferric sulfate coagulation, Fenton and sedimentation process, J. Hazard. Mater. 168 (2009) 1264–1268.

[6] M. Fan, R.C. Brown, S.W. Sung, C.-P. Huang, S.K. Ong, J.H. van Leeuwen, Comparisons of polymeric and conventional coagulants in arsenic (V) removal, Water Environ. Res. 75 (2003) 308–313.

[7] Y.H. Shi, M.H. Fan, R.C. Brown, S.W. Sung, J. Van Leeuwen, Comparison of corrosivity of polymeric sulfate ferric and ferric chloride as coagulants in water treatment, Chem. Eng. Process. 43 (2004) 955–964.

[8] K.E. Lee, N. Morad, T.T. Teng, B.T. Poh, Development, characterization and the application of hybrid materials in coagulation/flocculation of wastewater: a review, Chem. Eng. J. 203 (2012) 370–386.

[9] H.T. Wang, J. Qi, A.A. Keller, M. Zhu, F.T. Li, Effects of pH, ionic strength and humic acid on the removal of TiO2 nanoparticles from aqueous phase by coagulation, Colloid Surf. A 450 (2014) 161–165.

[10] A.K. Verma, R.R. Dash, P. Bhunia, A review on chemical coagulation/flocculation technologies for removal of colour from textile wastewaters, J. Environ. Manage. 93 (2012) 154–168.

[11] P.M. Teh, K.P.Y. Budiman, Recent advancement of coagulation–flocculation and its application in wastewater treatment, Ind. Eng. Chem. 55 (2016) 4363–4389 (Res).

[12] Y. He, F. Li, J.-Q. Jiang, Preparation and application of polyferric sulfate in drinking water treatment, in: The 12th International Conference on Environmental Science and Technology, Rhodes, Greece, 2011.

[13] W.P. Cheng, F.H. Chi, A study of coagulation mechanisms of polyferric sulfate reacting with humic acid using a fluorescence-quenching method, Water Res. 36 (2002) 4583–4591.

[14] R.M. Wang, Y. Wang, Y.F. He, F.Y. Li, Y. Zhou, N.P. He, Preparation of solid composite polyferric sulfate and its flocculation behavior for wastewater containing high concentration organic compounds, Water Sci. Technol. 61 (2010) 2749–2757.

[15] S. Zhao, G. Huang, H. Fu, Y. Wang, Enhanced coagulation/flocculation by combining diatomite with synthetic polymers for oily wastewater treatment, Sep. Sci. Technol. 49 (2014) 999–1007.

[16] Y. Wei, X. Dong, A. Ding, D. Xie, Characterization and coagulation-flocculation behavior of an inorganic polymer coagulant -poly-ferric-zinc-sulfate, J. Taiwan Inst. Chem. Eng. 58 (2016) 351–356.

[17] Q. Chang, H.Y. Wang, Preparation of PFS coagulant by sectionalized reactor, J. Environ. Sci. 14 (2002) 345–350.

[18] Q. Chang, Oxidation rate in the preparation of polyferric sulfate coagulant, J. Environ. Sci. 13 (2001) 104–107.

[19] Y.J. Zheng, Z.Q. Gong, B.Z. Chen, L.H. Liu, Preparation of solid polyferric sulfate from pyrite cinders and its structure feature, Trans. Nonferrous Met. Soc. China 13 (2003) 690–694.

[20] Y. Zeng, J. Park, Characterization and coagulation performance of a novel inorganic polymer coagulant-poly-zinc-silicate-sulfate, Colloid Surf. A 334 (2009) 147–154.

[21] T. Sun, L.L. Liu, L.L. Wan, Y.P. Zhang, Effect of silicon dose on preparation and coagulation performance of poly-ferric-aluminum-silicate-sulfate from oil shale ash, Chem. Eng. J. 163 (2010) 48–54.

[22] H.L. Zheng, H.L. Fang, S.J. Jiang, C. Yang, J.Y. Ma, Z.Q. Zhang, Preparation and structural analysis of diatomite-supported SPFS flocculant, Spectrosc. Spect. Anal. 31 (2011) 1917–1921.

[23] R.L. Frost, S.J. Palmer, J. Kristóf, E. Horváth, Thermoanalytical studies of silver and lead jarosites and their solid solutions, J. Therm. Anal. Calorim. 101 (2010) 73–79.

[24] H.J. Spratt, Structural Effects of Ammonium and Hydronium in Jarosite Minerals, School of Chemistry, Physics & Mechanical Engineering, Queensland University of Technology, 2015.

[25] H. Spratt, L. Rintoul, M. Avdeev, W. Martens, The thermal decomposition of hydronium jarosite and ammoniojarosite, J. Therm. Anal. Calorim. 115 (2014) 101–109.

[26] J.M. Kotler, N.W. Hinman, C.D. Richardson, J.R. Scott, Thermal decomposition behavior of potassium and sodium jarosite synthesized in the presence of methylamine and alanine, J. Therm. Anal. Calorim. 102 (2010) 23–29.

[27] C. Drouet, A. Navrotsky, Synthesis characterization, and thermochemistry of K-Na-H3O jarosites, Geochim. Cosmochim. Acta 67 (2003) 2063–2076.

[28] H. Wang, J.M. Bigham, O.H. Tuovinen, Formation of schwertmannite and its transformation to jarosite in the presence of acidophilic iron-oxidizing microorganisms, Mater. Sci. Eng. C 26 (2006) 588–592.